

Transition from the Bose gas to the Fermi gas through a Nuclear Halo

V.P. Maslov *

Abstract

The first part of the paper deals with the behavior of the Bose–Einstein distribution as the activity $a \rightarrow 0$. In particular, the neighborhood of the point $a = 0$ is studied in great detail, and the expansion of both the Bose distribution and the Fermi distribution in powers of the parameter a is used.

This approach allows to find the value of the parameter a_0 , for which the Bose distribution (in the statistical sense) becomes zero.

In the second part of the paper, the process of separation of a nucleon from the atom’s nucleus is studied from the mathematical point of view. At the moment when the nucleon tears away from the fermionic nucleus, the nucleus becomes a boson. We investigate the further transformations of bosonic and fermionic separation states in a small neighborhood of the pressure P equal to zero. We use infinitely small quantities to modify the parastatistical distribution. Our conception is based on interpolation formulas yielding expansions in powers of the density. This method differs from those in other models based on the interaction potential between two or three particles.

We obtain new important relations connecting the temperature with the chemical potential during the separation of a nucleon from the atom’s nucleus. The obtained relations allow us to construct, on an antipode of sorts of the Hougén–Watson P–Z chart, the very high temperature isotherms corresponding to nuclear matter. We call a new diagram a–Z chart. It is proved mathematically that the passage of particles satisfying the Fermi–Dirac distribution to the Bose–Einstein distribution in the neighborhood of pressure P equal to zero occurs in a region known as the “halo”.

We have obtained a new table for nuclear physics which demonstrates a monotonic relation between the nucleus mass number A , the binding energy E_b , the minimum value of activity $a = a_0$, the chemical potential $\mu_0 = T \log a_0$, the compressibility factor $F = PV/NT$ for a_0 , and also the minimum value of mean square fluctuation $\delta\mu_{min} = T/\delta N \leq \delta\mu$. The values $\delta\mu_{min}$ and δN are involved in uncertainty relations of nuclear physics.

1 Statistical transition of the Bose gas to the Fermi gas

1. It is well known that a Bose particle consists of two bound Fermi particles. For a Bose particle to become a Fermi particle, it is necessary that one of the Fermi particles forming the Bose particle must be “pushed out” *beyond* the volume V under consideration (in the

*National Research University Higher School of Economics, Moscow, 123458, Russia; Moscow State University, Physics Faculty, Moscow, 119234, Russia

two-dimensional case, V is the area) under the action of some energy. In the case of the volume of a ball (the area of a disk), the radius r is the radius of the “shell,” outside which the “entanglement” of two fermions into one boson terminates according to the Einstein–Podolsky–Rosen concept.

Let there be given a macroscopic volume V of radius at least 1 mm filled completely with a Bose gas (for example, helium-4) for the activity $a = 1$, i.e., on the caustic. We shall determine what amount of energy is required to “push out” one fermion from the specific volume under consideration. To obtain the total energy, i.e., the energy needed for the Bose gas (for example, helium-4) to go over completely into the Fermi gas (for example, helium-3), we must multiply the resulting quantity by the number of particles in the gas. It is the amount of energy required for the transition of the Bose gas to the Fermi gas that is the subject of the present study. In particular, we shall show that, for the number of degrees of freedom $D > 2$, we will have a jump of the energy E at the point $E = 1/\log a$ for $a = 0$, where a is the activity,

Remark 1. “The barrier” formed by the shell is described by a Bardeen–Cooper–Schrieffer type equation for Cooper pairs [1]–[2]. Since the volume under consideration is macroscopic (at least 1 mm³), by statistical calculations, the shell far exceeds the volume of the nucleus.

In our conception, we use the polylogarithm. The polylogarithm is determined by the activity a and the number of degrees of freedom D , where $D = 2\gamma + 2$ and γ is an auxiliary parameter. In the two-dimensional case, $\gamma = 0$, while, in the general number theory, $\gamma \leq 0$. The positive value $\gamma > 0$ corresponds to the gas state in classical thermodynamics and $\gamma < 0$, to the liquid state.

Both parameters a and D are dimensionless, while the volume V is a dimensional parameter. The dimensionless small parameter

$$\frac{\hbar^2}{mVT} \tag{1}$$

for $\gamma = 0$ (in the two-dimensional case, V is the area) corresponds to the semiclassical approximation in the sense that the semiclassical asymptotics is expanded in terms of this parameter. Therefore, as a rule, a parameter λ is also added so that the multiplicative term before the polylogarithm becomes dimensionless. Statistical quantities divided by the number of particles i.e., belonging to one particle, are called *specific quantities*: V/N is the *specific volume* and E/N is the *specific energy*. We proceed as follows: first, we shall find the specific energy and, further, we shall multiply it by the number of particles on the caustic $a = 1$.

The quantity $PV/(NT)$, where P is the pressure and T is the temperature, is dimensionless. It is called the *compressibility factor*. The temperature T in the two-dimensional case is determined from the relation $M = T \operatorname{Li}_2(a)$, where $a = 1$, as

$$T = \sqrt{\frac{M}{\zeta(2)}}, \tag{2}$$

where $\zeta(\cdot)$ is the Riemann zeta-function.

For the number of degrees of freedom $D > 2$, the density of the Bose gas at the point $a = 0$ vanishes as $1/|\log a|$ and behaves as $1/\log a$ for the Fermi gas (see below), just as the energy E of the Bose gas. The coefficient of $1/\log a$ for the energy of the Bose gas allows us to determine the energy needed for “all” the Bose particles to go over into Fermi particles.

The hidden parameter appearing in the Einstein–Podolsky–Rosen paradox could unite quantum and classical mechanics in the sense defined by the author; it can be obtained from

the general arguments in the first chapter of the book [3]. After Sec. 4 “Role of Energy,” the most important notion of time is introduced in Sec. 5 “Statistical Matrix.” Since, in the present paper, we calculate the statistical energy ΔE required for the transition of the Bose gas into the Fermi gas, it follows that by using Sec. 5 of the book [3] we can also calculate the statistical time

$$\Delta t \sim \frac{\hbar}{\Delta E}, \quad (3)$$

given by the authors of [3] to explain the transition to macroscopic physics. From the point of view of the metamathematical hidden parameter, this time plays a role similar to that of the mean free time in classical mechanics.

Let k denote the maximal admissible number of particles that can occupy one energy level, and let N_i denote the number of particles located at the i th energy level ¹. The number k is the maximal number of particles located at one energy level of a quantum operator of the Hamiltonian \hat{H} . For a Bose systems, it is obvious that $N_i \leq N$. Therefore, for a Bose system, $k \leq N$.

On the other hand, the number N_i is arbitrarily large, more precisely, maximally large, in view of the inequality $N_i \leq N$. This implies that $k = N$, and we obtain an equation for N in which, on the left-hand and right-hand sides, we have N from the formula for the Gentile parastatistics (see Sec. 4 below).

2. To find the energy that is of interest to us (the energy of transition of Bose particles to Fermi particles), it suffices to study the transition at the point $a = 0$. If we wish to widen the interval of the jump from the Bose distribution to the Fermi distribution, then we must use parastatistics, or Gentile statistics [6] in which the first term in parentheses gives the distribution for Bose particles and the other term, the parastatistical correction. The corresponding formula in the three-dimensional case is of the form (see [7])

$$N = \lambda \left\{ \int_0^\infty \frac{p^2 dp}{\exp\{p^2/2mT\} - 1} - (k + 1) \int_0^\infty \frac{p^2 dp}{\exp\{(k + 1)p^2/2mT\} - 1} \right\}. \quad (4)$$

For the Bose–Einstein distribution in the case of D degrees of freedom the following formulas are valid:

$$E = T\Phi(\gamma + 1)Li_{2+\gamma}(a), \quad N = \Phi Li_{1+\gamma}(a). \quad (5)$$

Here and elsewhere, $\gamma = D/2 - 1$, T is the temperature, $a = e^{\mu/T}$ is the activity, μ is the chemical potential,

$$\Phi = \left(\frac{\sqrt{2\pi mT}}{2\pi\hbar} \right)^{2(\gamma+1)} V,$$

where m is the mass of one particle, V is the volume of the system of particles, and \hbar is the Planck constant.

For the Fermi–Dirac distribution, the following formulas hold:

$$E = -T\Phi(\gamma + 1)Li_{2+\gamma}(-a), \quad N = -\Phi Li_{1+\gamma}(-a). \quad (6)$$

As we see, formulas (5) and (6) differ by sign; therefore, the activity a passes through the point $a = 0$.

¹For the transition from a discrete spectrum to a continuous one with respect to the parameter V , see [4], [5].

In the case of parastatistics, i.e., there are at most k particles at each level, the following relations hold:

$$E = \Phi T(\gamma + 1)(\text{Li}_{2+\gamma}(a) - \frac{1}{(k+1)^{\gamma+1}}\text{Li}_{2+\gamma}(a^{k+1})), \quad (7)$$

$$N = \Phi(\text{Li}_{1+\gamma}(a) - \frac{1}{(k+1)^\gamma}\text{Li}_{1+\gamma}(a^{k+1})). \quad (8)$$

According to the conventional definitions, for $k = 1$, we have the Fermi case and, for $k = \infty$, the Bose case.

Let us consider another important dimensionless quantity, which was mentioned above, namely, the compressibility factor defined by the formula $Z = PV/NT$.

The following thermodynamic relation is well known:

$$E = -(\gamma + 1)\Omega = PV(\gamma + 1) \quad (9)$$

As is seen from relation (9), PV is expressed in terms of E ; therefore, the compressibility factor can be expressed in terms of the polylogarithm. For the Bose case, the compressibility factor takes the form

$$Z|_{\text{Bose}} = \frac{\text{Li}_{2+\gamma}(a)}{\text{Li}_{1+\gamma}(a)} \quad (10)$$

and, for the Fermi case, we have

$$Z|_{\text{Fermi}} = \frac{\text{Li}_{2+\gamma}(-a)}{\text{Li}_{1+\gamma}(-a)}. \quad (11)$$

For the Gentile statistics with parameter k , we have the following expression for the compressibility factor:

$$Z|_k = \frac{\text{Li}_{2+\gamma}(a) - \frac{1}{(k+1)^{\gamma+1}}\text{Li}_{2+\gamma}(a^{k+1})}{\text{Li}_{1+\gamma}(a) - \frac{1}{(k+1)^\gamma}\text{Li}_{1+\gamma}(a^{k+1})}. \quad (12)$$

3. The compressibility factor Z multiplied by the temperature T is the specific energy. To obtain the jump of the specific energy, it suffices to consider the jump of the compressibility factor from the Fermi system to the Bose system.

The following representation for the polylogarithm is known:

$$\text{Li}_s(a) = \sum_{i=1}^{\infty} \frac{a^i}{i^s}; \quad (13)$$

substituting this expression into (10), (11), (12), we obtain the following expansions of the compressibility factor:

$$\begin{aligned} Z|_{\text{Fermi}} &= 1 + a2^{-\gamma-2} - a^22^{-2\gamma-3}3^{-\gamma-2}(2^{2\gamma+4} - 3^{\gamma+2}) \\ &\quad - a^32^{-3\gamma-4}3^{-\gamma-2}(7 \cdot 2^{2\gamma+2} - 3^{\gamma+2} - 2\gamma3^{\gamma+3}) \\ &\quad - a^42^{-4\gamma-5}3^{-2\gamma-3}5^{-\gamma-2}(2^{4\gamma+7}3^{2\gamma+3} - 2^{4\gamma+6}5^{\gamma+2} - 3^{2\gamma+3}5^{\gamma+2} + 2^{2\gamma+3}3^{\gamma+1}5^{\gamma+3} - 2\gamma3^{2\gamma+3}5^{\gamma+3}) \\ &\quad + O(a^5), \end{aligned} \quad (14)$$

$$\begin{aligned} Z|_{\text{Bose}} &= 1 - a2^{-\gamma-2} - a^22^{-2\gamma-3}3^{-\gamma-2}(2^{2\gamma+4} - 3^{\gamma+2}) \\ &\quad + a^32^{-3\gamma-4}3^{-\gamma-2}(7 \cdot 2^{2\gamma+2} - 3^{\gamma+2} - 2\gamma3^{\gamma+3}) \\ &\quad - a^42^{-4\gamma-5}3^{-2\gamma-3}5^{-\gamma-2}(2^{4\gamma+7}3^{2\gamma+3} - 2^{4\gamma+6}5^{\gamma+2} - 3^{2\gamma+3}5^{\gamma+2} + 2^{2\gamma+3}3^{\gamma+1}5^{\gamma+3} - 2\gamma3^{2\gamma+3}5^{\gamma+3}) \\ &\quad + O(a^5). \end{aligned} \quad (15)$$

The jump of the compressibility factor is expressed as (see Fig. 1):

$$\Delta Z(a) = Z|_{K=1} - Z|_{\text{Bose}} = \frac{a}{2^{\gamma+1}} + O(a^2), \quad (16)$$

while the jump of the *specific* energy E_{spec} is of the form

$$\Delta E_{\text{spec}}(a) = T(\gamma + 1)\Delta Z(a) = T(\gamma + 1)\frac{a}{2^{\gamma+1}} + O(a^2). \quad (17)$$

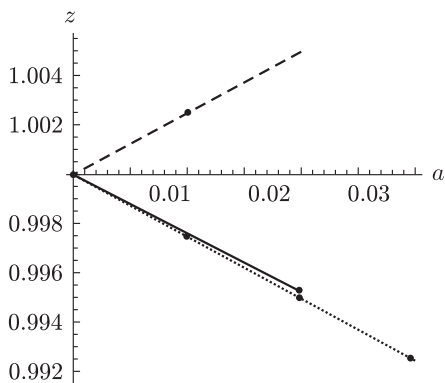


Figure 1: Dependence of the compressibility factor Z on the activity a for the two-dimensional case. Here $\Phi = 100$, $\gamma = 0$. The upper (dashed) curve corresponds to the Fermi system. The middle (solid) curve corresponds to the Bose system up to $O(a^2)$. The lower (dotted) curve corresponds to the exact Bose system. The points on the curves correspond integer N .

The dependence of the compressibility factor Z on the activity a for the case $\gamma = 0$ is shown in Fig. 1.

4. As indicated above, the author obtained a self-consistent equation in which N is an unknown quantity. We are interested in the point at which the number of Bose particles N is 0, i.e., the point at which Bose particles vanish. An example of this point is given in Fig. 2. Let us note that the value of the activity a is not zero at this point; it depends essentially on the function Φ and the parameter γ . Let us consider successively the cases of small N , $\gamma \geq 0$, and $\gamma < 0$.

4.1. As pointed out above, there can be at most N particles at each energy level. Therefore, for the Bose system, we put $k = N$. Equation (8) takes the form:

$$N = \Phi(Li_{1+\gamma}(a) - \frac{1}{(N+1)^\gamma} Li_{1+\gamma}(a^{N+1})). \quad (18)$$

Expanding the right-hand side of Eq. (18) in the small parameter $N \ll a$, we obtain

$$\begin{aligned} N = & \Phi N(\gamma Li_{\gamma+1}(a) - \log(a) Li_\gamma(a)) \\ & + \frac{1}{2} W N^2 (\log^2(a)(-Li_{\gamma-1}(a)) - \gamma((\gamma+1) Li_{\gamma+1}(a) - 2 \log(a) Li_\gamma(a))) + o((\log a N)^2). \end{aligned} \quad (19)$$

Remark 2. We deal with two double limits. The first case is

$$\lim_{a \rightarrow 0} a \lim_{N \rightarrow 0} N.$$

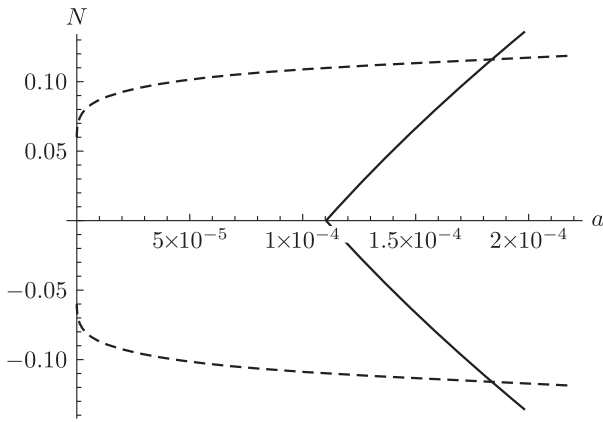


Figure 2: Dependence $N(a)$ for $W = 1000$, where $W = V(\lambda^2 T)^{\gamma+1}$, λ is the parameter depending on the mass, and $\gamma = 0$. The dotted curve corresponds to $N = -1/\log(a)$. The solid line corresponds to $N = 0$.

In this case, $N \ll a$, and we obtain some value of a_0 for which the number of Bose particles of the distribution $N = 0$.

In the second case, N is fixed and $a \ll N$. As a result, the Gentile parastatistical term vanishes.

If, in the expansion (18), we take into account the terms up to the second order of smallness inclusive, then we can obtain the equation for N whose solution is as follows:

$$N = 2 \frac{\gamma \Phi \text{Li}_{\gamma+1}(a) - \Phi \log(a) \text{Li}_{\gamma}(a) - 1}{\Phi(\log^2(a) \text{Li}_{\gamma-1}(a) + \gamma((\gamma+1) \text{Li}_{\gamma+1}(a) - 2 \log(a) \text{Li}_{\gamma}(a)))}. \quad (20)$$

Equation (20) yields the following equation for a_0 in the case $N = 0$:

$$\gamma \Phi \text{Li}_{\gamma+1}(a_0) - \Phi \log(a_0) \text{Li}_{\gamma}(a_0) - 1 = 0, \quad (21)$$

For small a_0 , the following asymptotic formula holds:

$$\Phi = -\frac{1}{a_0 \ln a_0}, \quad (22)$$

or

$$\Phi = \frac{1}{a_0 \ln \Phi}. \quad (23)$$

We obtain

$$\Delta Z(a_0) = \frac{a_0}{2^{\gamma+1}} = -\frac{1}{2^{\gamma+1} \Phi \ln a_0}. \quad (24)$$

The maximal number of particles N_c in the system is at the caustic point $a = 1$. The value of N_c is given by

$$N_c = \Phi \left(\text{Li}_{1+\gamma}(1) - \frac{1}{(N_c + 1)^\gamma} \text{Li}_{1+\gamma}(1) \right). \quad (25)$$

We shall use the integral representation of the polylogarithm Li , obtaining

$$N_c = \Phi \beta \int_0^\infty \left(\frac{1}{\exp\{\varepsilon/T\} - 1} - \frac{N_c + 1}{\exp\{(N_c + 1)\varepsilon/T\} - 1} \right) d\varepsilon, \quad \beta = 1/T. \quad (26)$$

4.2. Consider the case $D = 2$. Let $N = N_c$ be the solution of Eq. (26). We shall evaluate the integral in (26) (with the same integra) taken from δ to ∞ and then pass to the limit as $\delta \rightarrow 0$. After making the change $\beta x = \xi$ in the first term and $\beta(N_c + 1)x = \xi$ in the second term, where $\beta = 1/T$, we obtain

$$N_c = \Phi \int_{\delta\beta}^{\infty} \frac{d\xi}{e^\xi - 1} - \Phi \int_{\delta\beta(N_c+1)}^{\infty} \frac{d\xi}{e^\xi - 1} + O(\delta) = \Phi \int_{\delta\beta}^{\delta\beta(N_c+1)} \frac{d\xi}{e^\xi - 1} + O(\delta) \quad (27)$$

$$\sim \Phi \int_{\delta\beta}^{\delta\beta(N_c+1)} \frac{d\xi}{\xi} + O(\delta) = \Phi \{\ln(\delta\beta(N_c + 1)) - \ln(\delta\beta)\} + O(\delta) = \Phi \ln(N_c + 1) + O(\delta). \quad (28)$$

In the three-dimensional case, this formula is of the form (4).

After passing to the limit as $\delta \rightarrow 0$, we obtain

$$N_c = \Phi \log(N_c + 1). \quad (29)$$

Multiplying the difference of the specific energies $\Delta E_{\text{spec}}(a_0)$ by the number of particles defined by formula (25), we obtain the difference of the energies for the whole system of particles in the units of T in the case $\gamma > 0$:

$$\Delta E = \Delta E_{\text{spec}}(a_0) N_c = \frac{\gamma + 1}{2^{\gamma+1} \ln \Phi} Li_{1+\gamma}(1) \left(1 - \frac{1}{(N_c + 1)^\gamma}\right) \quad (30)$$

and, in the case $\gamma = 0$, we have

$$\Delta E = \Delta E_{\text{spec}}(a_0) N_c = \frac{1}{2 \ln \Phi} \log(N_c + 1), \quad (31)$$

where N_c can be calculated from formula (25) (which contains Φ).

4.3. Let us pass to the case $\gamma < \gamma_0 < 0$, i.e., $D < D_0 < 2$.

For the case in which $\gamma < \gamma_0 < 0$, the following lemma holds.

Lemma 1. *Consider the integral*

$$N = B \int_0^\infty \left(\frac{1}{e^{\beta x - \beta \mu} - 1} - \frac{k}{e^{k(\beta x - \beta \mu)} - 1} \right) x^\gamma dx, \quad (32)$$

where $-1 < \gamma < \gamma_0 < 0$, and $B > 0$ and $k > 0$ are constants.

Then

$$N = -\frac{B}{\beta^{\gamma+1}} c_{\beta\mu,\gamma} + \frac{Bk^{-\gamma}}{\beta^{\gamma+1}} c_{k\beta\mu,\gamma}, \quad (33)$$

where

$$c_{\mu,\gamma} = \int_0^\infty \left(\frac{1}{\xi - \mu} - \frac{1}{e^{\xi - \mu} - 1} \right) \xi^\gamma d\xi. \quad (34)$$

By the Lemma, Eq. (19) takes the form

$$N_c = \Phi C(\gamma) (-1 + (N_c + 1)^{-\gamma}), \quad (35)$$

where

$$C(\gamma) = \frac{1}{\Gamma(\gamma + 1)} \int_0^\infty \left(\frac{1}{\xi} - \frac{1}{e^\xi - 1} \right) \xi^\gamma d\xi. \quad (36)$$

As $N_c \rightarrow \infty$, we can neglect the summand -1 in formula (35) as well as 1 compared to N_c , whence we obtain

$$N_c = \Phi C(\gamma) N_c^{-\gamma}, \quad (37)$$

$$N_c = (\Phi C(\gamma))^{1/(\gamma+1)} = T \left(\left(\frac{\sqrt{2\pi m}}{2\pi\hbar} \right)^{2(\gamma+1)} VC(\gamma) \right)^{1/(\gamma+1)}; \quad (38)$$

as a final result, we arrive at the expression

$$N_c = T(VC(\gamma))^{1/(\gamma+1)} \left(\frac{\sqrt{2\pi m}}{2\pi\hbar} \right)^2. \quad (39)$$

For the jump of the energy, we obtain the expression

$$\Delta E = \frac{\gamma + 1}{2^{\gamma+1} \Phi \ln \Phi} (\Phi C(\gamma))^{1/(\gamma+1)} = \frac{\gamma + 1}{2^{\gamma+1} \ln \Phi} C(\gamma)^{1/(\gamma+1)} \Phi^{-\gamma/(\gamma+1)}. \quad (40)$$

2 Using infinitesimal quantities to describe the separation process of neutrons from atomic nuclei

A Bose particle consists of two Fermi particles which are linked together by an interaction force or, as it is customary to say at the present time, by an entangling force. Sometimes the two fermions constituting the boson are absolutely identical. They cannot be distinguished or numbered. Sometimes the fermions differ in mass, then they can be distinguished. For example, a proton and an electron are fermions of different mass, and together they constitute a pair – a boson. Such fermions can be distinguished and numbered, using the mechanism of numeration theory. While if the masses of the particles approach each other and coincide in the limit, then we cannot distinguish them.

The passage from the case of distinguishable particles to the case when the particles become undistinguishable leads to other quantum-mechanical formulas and therefore, to different commutation relations [8].

The separation of a fermion from the nucleus and the capture of a fermion is a very rapid process. The question of the possibility of monitoring that transformation as if it occurred in slow motion arises. Mathematically, this means that we must use such tools which may be applied to both fermions and bosons.

In the present paper we use infinitely small quantities to modify the parastatistical distribution (the Gentile statistical method). This approach allows to apply the “antipod” of the P-Z chart corresponding to the Van-der-Waals equation of state in thermodynamics, also known as the Hougen–Watson chart. In this antipode, the isotherms under consideration, unlike those in the Van-der-Waals model, correspond to extremely high temperatures, which increase even more when the compressibility factor Z decreases.

The obtained antipode of the P-Z chart adequately corresponds to the behavior of nuclear matter. We will show in this paper that the passage of particles satisfying the Fermi–Dirac distribution to the Bose–Einstein distribution in the neighborhood of pressure P equal to zero occurs in a region known as the “halo”. This region is different for various isotopes and depends on chemical potentials.

The method developed in this paper differs from those in other models based on the interaction of two or three particles, such as the Faddeev–Skyrme model or models involving the Lennard–Jones potential. This method is based on interpolation formulas yielding

expansions in powers of the density. Just as in the Van-der-Waals interpolation formula, the zeroth approximation is given by ideal gas, whereas in models based on potentials the zeroth approximation is given by the zero potential.

Niels Bohr in 1936 proposed one of the earliest models of the atomic nucleus in the framework of the theory of compound nucleus [9]. Later, by Carl Weizsäcker was obtained a semi-empirical formula for the binding energy of the atomic nucleus E_c :

$$E_c = \alpha A - \beta A^{2/3} - \gamma \frac{Z^2}{A^{1/3}} - \varepsilon \frac{(A/2 - Z)^2}{A} + \delta, \quad (41)$$

where

$$\delta = \begin{cases} +\chi A^{-3/4} & \text{for even-even nuclei,} \\ 0 & \text{for nuclei with odd } A, \\ -\chi A^{-3/4} & \text{for odd-odd nuclei,} \end{cases}$$

A is the mass number (total number of nucleons) in the nucleus, Z is the charge number (number of protons) in the nucleus, and α , β , γ , ε , and χ are parameters obtained by statistical treatment of experimental data. This formula provides sufficiently exact values of the binding energies and masses for many nuclei, which permits using it to analyze different properties of the atomic nucleus.

In this paper we obtain new important relations between the temperature and the chemical potential in the process of nucleon separation from the atomic nucleus. For this, we use the parastatistic relations modified by the mathematical notion of infinitesimals.

2.1 New parastatistics

Let us assume that the energy of each of the particles takes one of the values of the given discrete spectrum. We shall denote by N_i the number of particles located at the i -th level energy.

Besides the Bose–Einstein and Fermi–Dirac statistics, physicists use parastatistics (aka Gentile statistics [6]) that generalizes the two previously mentioned statistics, which are thus particular cases of parastatistics. According to the latter, as it was said earlier, at each energy level, there may be no more than K particles. By the usual definitions, the Fermi case is realized for $K = 1$. In the case of Bose statistics $N_i \leq N$ because then $\sum_i N_i = N$, implies that $K = N$.

We will be dealing with infinitely small K and N equal to each other. General approach see in [10].

In the case of parastatistics, we have the following relations, in which the first term in parentheses gives the distribution for Bose particles, and the second term, the parastatistical correction (compare (7)-(8)):

$$E = \frac{V}{\lambda^D} T(\gamma + 1) \left(\text{Li}_{2+\gamma}(a) - \frac{1}{(K + 1)^{\gamma+1}} \text{Li}_{2+\gamma}(a^{K+1}) \right), \quad (42)$$

$$N = \frac{V}{\lambda^D} \left(\text{Li}_{1+\gamma}(a) - \frac{1}{(K + 1)^\gamma} \text{Li}_{1+\gamma}(a^{K+1}) \right), \quad (43)$$

where $\text{Li}_{(\cdot)}(\cdot)$ is the polylogarithm function, $a = e^{\mu/T}$ is the activity (μ being the chemical potential, T being the temperature), $\gamma = D/2 - 1$, D is the number of degrees of freedom (the dimension), λ is the de Broglie wavelength:

$$\lambda = \sqrt{\frac{2\pi\hbar^2}{mT}}, \quad (44)$$

where \hbar is the Planck constant, m the mass of one particle.

The de Broglie wavelength is related to the Bohr–Sommerfeld quantization condition, i.e., to the quantization of the angular momentum (see [11] and related works, in particular [12]–[18]).

2.2 Passage from the Bose-type region to the Fermi-type region through a nuclear halo

Before completely separating from a nucleus, a nucleon stays within an area around a nucleus where it is bound to a nucleus with entanglement forces. In this area the probability to discover a neutron is higher than the probability to discover a proton. It is well-known that the area where the density distribution of neutrons much exceeds the density distribution of protons is called a nuclear halo.

The neutron halo in atomic nuclei is defined as an extended distribution of neutron density and a narrow momentum distribution of fragmentation products [19]. Here the uncertainty principle manifests itself: when the distribution in space is wide, then the momentum distribution is narrow.

We will call the area similar to a nuclear halo a *region of uncertainty*. As shown in this paper, the width of the region of uncertainty is determined by the value of the chemical potential μ : the larger is the value of the chemical potential, the narrower is the region of uncertainty. For those elements whose chemical potential is close to zero, the width of the halo tends to infinity.

This can be explained as follows. The number of particles N is a conjugate value to the chemical potential. For these values the statistical analogue of the Heisenberg uncertainty principle is valid (see [20]):

$$\Delta\mu_0\Delta N \geq T. \quad (45)$$

In the case when $\Delta\mu_0 = -\infty$, the number of particles is known. However in the case when the value $\Delta\mu_0$ is finite, for number of particles N there exists a finite uncertainty value ΔN . When $\Delta\mu_0 \rightarrow 0$, the value ΔN tends to infinity and corresponds to the infinitely wide region of uncertainty.

The region corresponding to the difference of pressure $P = 0$ and to an infinitely small sequence $\{P_K\} \rightarrow 0$ constitutes the nuclear halo, or the region of uncertainty. The passage from the Bose-type region to the Fermi-type region occurs through the nuclear halo, which contains the value of the pressure $P = 0$. We denote by a_0 the maximal value of the activity a for Bose particles as $N \rightarrow 0$. The quantity a_0 indicates the maximal value of the activity at which the decomposition of bosons into fermion occurs.

Let us recall some definitions and relationships that we used in the paper [21]. It will be helpful to consider more general cases later in this work.

For an ideal gas of dimension $D = 3$, relations (42), (43) become

$$N = \frac{V}{\lambda^3}(\text{Li}_{3/2}(a) - \frac{1}{(K+1)^{1/2}} \text{Li}_{3/2}(a^{K+1})), \quad (46)$$

$$E = \frac{3}{2} \frac{V}{\lambda^3} T(\text{Li}_{5/2}(a) - \frac{1}{(K+1)^{3/2}} \text{Li}_{5/2}(a^{K+1})). \quad (47)$$

The expansion of the summand $\frac{1}{(K+1)^{1/2}} \text{Li}_{3/2}(a^{K+1})$ from formula (46) in small values of K has the form:

$$\frac{1}{(K+1)^{1/2}} \text{Li}_{3/2}(a^{K+1}) = \text{Li}_{3/2}(a) - [K(\text{Li}_{3/2}(a)/2 - \log(a) \text{Li}_{1/2}(a)) + O(K^2)]. \quad (48)$$

Let $B = V/\lambda^3 > 0$. Then equation (46) for small K acquires the form:

$$N = BK\left(\frac{1}{2}\text{Li}_{3/2}(a) - \log(a)\text{Li}_{1/2}(a)\right) + O(K^2). \quad (49)$$

In our considerations N is an infinitely small number, .. $N = \alpha_i$, where a sequence of infinitesimals $\alpha_i \rightarrow 0$ as $i \rightarrow \infty$. Similarly $K = \beta_i$, where a sequence of infinitesimals $\beta_i \rightarrow 0$ as $i \rightarrow \infty$. The sequences α_i and β_i are similar to each other, i.e. $\lim_{i \rightarrow \infty} \frac{\alpha_i}{\beta_i} = 1$. Thus we are not dealing with the Fermi statistics or the Bose statistics, but with a parastatistics of a new type, which can be called a Bose-like statistics.

Dividing both sides of (49) by N and taking the limit as $K \rightarrow 0$, yields an expression for a_0 , i.e., the value of a for which $K = N = 0$:

$$\frac{1}{2}\text{Li}_{3/2}(a_0) - \log(a_0)\text{Li}_{1/2}(a_0) - B^{-1} = 0. \quad (50)$$

Equation (50) in the case of an arbitrary coefficient $\gamma = D/2 - 1$ instead of $1/2$, after similar arguments, acquires the form:

$$\gamma\text{Li}_{\gamma+1}(a_0) - \log(a_0)\text{Li}_{\gamma}(a_0) - \frac{\lambda^{2(\gamma+1)}}{V} = 0. \quad (51)$$

Equation (51) has a unique solution $a_0 > 0$ that depends on B and γ .

In the case $K = N$, equation (46) acquires the form

$$N = B\left(\text{Li}_{3/2}(a) - \frac{1}{(N+1)^{1/2}}\text{Li}_{3/2}(a^{N+1})\right). \quad (52)$$

This equation obviously has the solution $N \equiv 0$ for any $a \geq 0$. However, for $a > a_0$, it has one more nonnegative solution $N(a)$. This can be verified by constructing the graphs of the right-hand and left-hand sides of (52) as a function of a for an arbitrary fixed $N > 0$. The right-hand side of the equation is zero for $a = 0$ and monotonically grows for $a \in (0, \infty)$, while the left hand side is a constant that does not depend on a .

Substituting the obtained relation $N(a)$ in formula (47), we can find the dependence $E(a)$, and with it the pressure $P(a)$, by using the relation

$$E = (\gamma + 1)PV. \quad (53)$$

Let us substitute the obtained relation into the graph of the compressibility factor

$$Z = PV/(NT) \quad (54)$$

as a function of P (this graph is known as the Hougen–Watson chart).

Now we place a minus sign before dependencies $P(a)$ and $N(a)$ for the Bose branch, i.e. these values are considered as negative. It follows from this that in the Bose-like region $Z(a) > 0$. We will refer to a new chart as the a-Z chart.

The value $a = a_0$ is the minimum value of activity for the Bose branch, since for $a < a_0$ the region of uncertainty occurs where $N \equiv 0$ and $P \equiv 0$ for all a up to the value of $a = 0$. Here the passage of particles to the Fermi branch begins.

For Fermi statistics in the case $D = 3$, we have the relations

$$N = -\frac{V}{\lambda^3}\text{Li}_{3/2}(-a), \quad (55)$$

$$E = -\frac{3}{2}\frac{V}{\lambda^3}T\text{Li}_{5/2}(-a). \quad (56)$$

Let us call the curve on the a-Z chart, constructed according to formulas (55)–(56) of Fermi statistics, the Fermi branch. The pressure P , as well as the number of particles N , on the Fermi branch is positive.

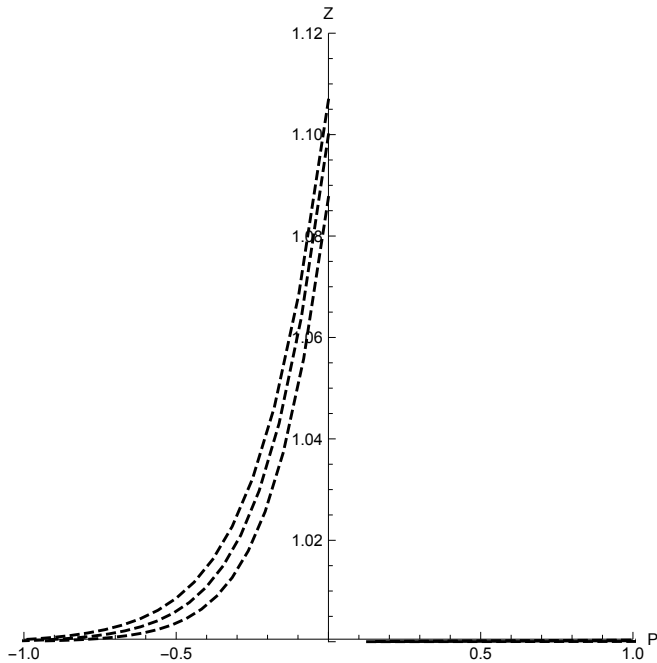


Figure 3: Dependence of the compressibility factor Z on the pressure P , expressed in the units MeV/fm^3 for carbon-12, nitrogen-14, fluorine-19 (from top to bottom). The continuous line represents the line $Z = 1$. It is the beginning of the Fermi branch. The hashed lines show isotherms of the Bose branch, constructed according to formulas (46)–(47). The temperature is equal to the nucleus binding energy E_b . The corresponding values of E_b and a_0 are given in Table 1 in Appendix.

2.3 a-Z chart for nuclear matter

The value of the activity a for a known value of the temperature T determines the corresponding value of the chemical potential

$$\mu = T \log(a). \quad (57)$$

In particular, for $a = a_0$, the higher the temperature, the smaller is a_0 , and the larger is the value of $|\mu_0|$. Thus, as the temperature grows, the point of passage μ_0 approaches the point $\mu = -\infty$ at which the pressure P changes sign (see [22]).

Table 1 in Appendix presents values of a_0 and $\mu_0 = T \log a_0$ for isotopes of stable chemical elements.

The value of a_0 in the case of separation can be found by means of formula (50), taking into account the expression of the de Broglie wavelength λ in terms of the volume V of the nucleus, its temperature T and its mass m . The volume of the nucleus is taken to be that of a ball of radius $r_0 = A^{1/3} 1.2 \times 10^{-15} \text{ m}^3$. The temperature T of the nucleus expressed in energy units is taken equal to the binding energy of the nucleus E_b , equal to the core temperature T (obtained from the database IsotopeData).

Table 1 demonstrates a monotonic relation between the nucleus mass number A , the binding energy E_b , the minimum value of activity $a = a_0$, the chemical potential $\mu_0 = T \log a_0$, and the compressibility factor $Z = PV/NT$ for a_0 .

We have obtained an equation (50) from which we can find the value of a_0 , and can determine the temperature T at which this value is attained.

Fig. 3 shows the dependence of the compressibility factor $Z = PV/(NT)$ on the pressure P , expressed in the units MeV/fm^3 carbon-12, nitrogen-14, fluorine-19. The dashed lines

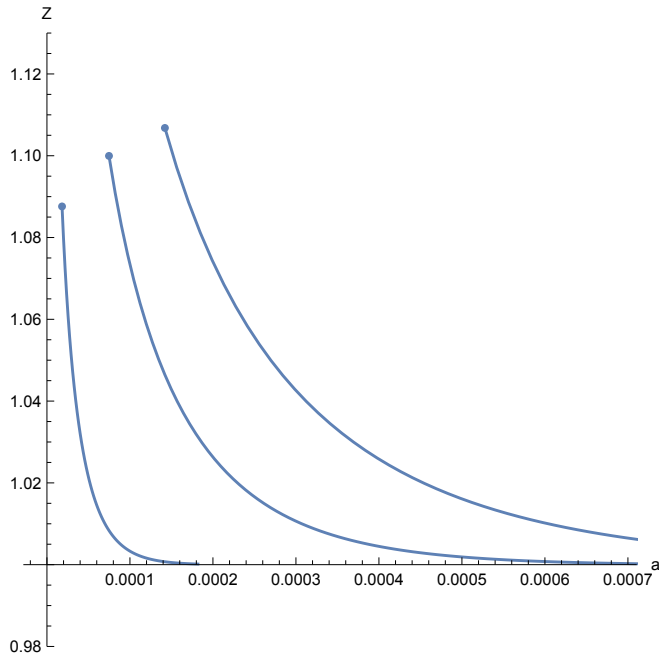


Figure 4: Dependence of the compressibility factor Z on the activity a , expressed in the units MeV/fm^3 for fluorine-19, nitrogen-14, carbon-12 (from left to right). The lines show isotherms of the Bose branch, constructed according to formulas (46)–(47). The temperature is equal to the nucleus binding energy E_b (see Table 1 in Appendix).

are the isotherms of the Bose branch constructed by means of formulas (46), (47), (54), and (53). The isotherms are parametric curves $P(a)$, $Z(a)$.

Let $\{P_K\}$ be an infinitely small sequence, coinciding with the infinitely small quantity K . It can be shown that the corresponding sequence $\{Z_k\}$ tends to a number greater than unity in the Bose-like region and to unity in the Fermi-like region (see Fig. 3).

The temperature is equal to the extremal value of the binding energy E_b , indicated in Table 1. To each value of a_0 there corresponds a definite value of the temperature T . In turn, to each value of T there corresponds an isotherm on the Hougén–Watson chart. These isotherms lie in the second quadrant. If the volume is constant, the temperature characterizing the isotherm becomes smaller as the point $a = a_0$ becomes nearer to $a = 1$.

Thus we can say that the Van-der-Waals isotherms are in a sense opposite to the isotherms of nuclear matter shown in Fig. 3.

This shows that the chemical potential μ at $P = 0$ does not become equal to minus infinity and so the axis Z at $P = 0$ is not the boundary between two unrelated structures. Since the value of $|\mu_0|$ is very large but not infinite between the values of the infinitely small quantities $\{P_K\}$ and the region obeying the Fermi–Dirac distribution, there is a “halo” dividing the Bose region from the Fermi region.

The value of the chemical potential μ_0 determines the halo width. The halo expands as μ_0 is close to zero. It can become infinitely large.

In the classical thermodynamics this situation corresponds to passing through the point where the pressure vanishes (i.e. passing from a negative compressibility factor Z to a positive Z). The halo is a region of indeterminacy: nobody knows what happens with the particles in the domain of a nuclear halo. We can refer to halo as the lacunary indeterminacy.

We do not consider the problem of proving that the isotherms on Fig. 3 exist. We give an approximate solution of the obtained equations (see similar approaches in papers [23], [24]), in which all the isotherms corresponding to different values of a_0 are approximately constructed.

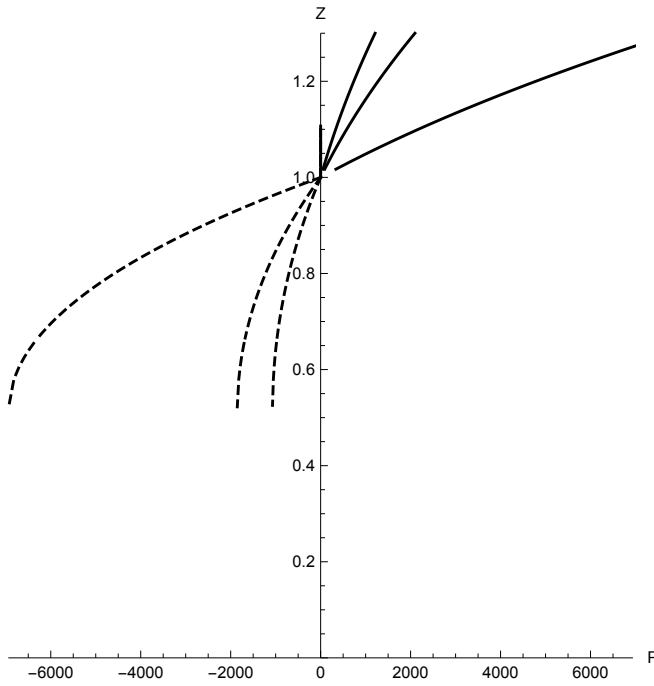


Figure 5: Dependence of the compressibility factor Z on the pressure P , expressed in the units MeV/fm^3 for fluorine-19, nitrogen-14, carbon-12 (from left to right in the region $P < 0$). The continuous line represents the Fermi branch. The hashed lines show isotherms of the Bose branch, constructed according to formulas (46)–(47).

In the point $a = 1$ (i.e. on the spinodal) the compressibility factor has the form:

$$Z_s = \frac{\zeta(5/2)}{\zeta(3/2)} \frac{1 - \frac{1}{(N_s+1)^{3/2}}}{1 - \frac{1}{(N_s+1)^{1/2}}}, \quad (58)$$

where N_s is determined from the relation

$$N_s = \frac{V}{\lambda^3} \zeta(3/2) \left(1 - \frac{1}{(N_s+1)^{1/2}} \right). \quad (59)$$

In the Fig. 4 upper ends of isotherms correspond to $a = a_0$. In the Fig. 3 corresponding points lie on the axis Z . This makes it possible to consider and compare behavior of isotherms of different chemical elements.

In Fig. 5 isotherms shown in Fig. 3 are drawn on a different scale.

One can see in Fig. 5 that the tangent to the lead curve in the bend point is parallel to the axis Z . This is a very important point where the activity $a = 1$. It connects the matter under consideration with the Van-der-Waals gas. This point is evidence of passing to the nuclear matter. Nuclear matter is a substance which in contrast to the nucleus has no boundaries. The bending down of the lead isotherm indicates that in the separation process of neutrons from an atomic nuclei we pass to another substance of nuclear matter.

Thus we have described a complete picture of passing from a substance which occurs when a neutron separates from an atomic nucleus to the nuclear matter substance.

Conclusion

We have shown that using infinitesimals N and K equally fast tending to zero leads to the determination of the value of a parameter a_0 that allows us to construct an antipode of sorts

of the Hougén–Watson P-Z chart for nuclear matter. We call a new diagram the a-Z chart. We have shown that, knowing the values of a_0 , we can construct all the isotherms on the a-Z chart. The smaller the value of a_0 the higher temperature of nuclear matter is.

In the paper it was shown that during separation of neutrons from atomic nuclei, between Bose-like and Fermi-like regions there exists a nuclear halo, or a region of uncertainty related to the chemical potential μ . The properties of halo may be used to model a medium for filtering radioactive elements. Such a filter turned out to be more efficient than the Darcy filtering medium used in the paper [25] (also see [26]).

The obtained in the paper rigorous mathematical approach unexpectedly yields a new picture, which adequately describes the passing to the nuclear matter during separation process of neutrons from atomic nuclei. This led to a new table for nuclear physics (see Appendix) which demonstrates a monotonic relation between the nucleus mass number A , the binding energy E_b , the minimum value of activity $a = a_0$, the chemical potential $\mu_0 = T \log a_0$, and the compressibility factor $Z = PV/NT$ for a_0 and also the minimum value of mean square fluctuation $\delta\mu_{min} = T/\delta N \leq \delta\mu$. The values $\delta\mu_{min}$ and δN are involved in uncertainty relations of nuclear physics.

References

- [1] G. V. Koval' and V. P. Maslov, "Ultrasecond quantization at temperatures distinct from zero," *Math. Notes* **82** (1) 52–57 (2007).
- [2] G. V. Koval' and V. P. Maslov, "Generalization of the Bardeen–Cooper–Schrieffer method for pair interactions," *Teoret. Mat. Fiz.* **154** (3) 495–502 (2008).
- [3] L. D. Landau and E. M. Lifshits, *Statistical Physics* (Fizmatlit, Moscow, 2013).
- [4] V. P. Maslov, *Perturbation Theory and Asymptotical Methods* (Izd. Moskov. Univ., Moscow, 1965; Dunod, Paris, 1972) [in Russian and French].
- [5] A. I. Shtern, "Remark concerning Maslov's theorem on homomorphisms of topological groups," *Russian J. Math. Phys.* **24** (2), 262–262 (2017).
- [6] W.-S. Dai and M. Xie, "Gentile statistics with a large maximum occupation number," *Ann. Phys.* **309**, 295–305 (2004).
- [7] I. A. Kvasnikov, *Thermodynamics and Statistical Physics: Theory of Equilibrium Systems* (URSS, Moscow, 2002), Vol. 2 [in Russian].
- [8] Salo, P. & Hietarinta, J. Ground state in the Faddeev-Skyrme model *Physical review D* **62** 081701(2000).
- [9] Bohr, N. Neutron capture and nucleus structure *Uspekhi Fiz. Nauk* **14** (4), 425–435 (1936).
- [10] Davis, M. & Hersh, R. Nonsrandard analysis *Scienific American* 226 (6), 78–86 (1972).
- [11] Litvinov, G. L. The Maslov dequantization, idempotent and tropical mathematics: a very brief introduction. *Contemp. Math.*, Vol. 377: *Idempotent Mathematics and Mathematical Physics* (Amer. Math. Soc., Providence, RI, 2005).

- [12] Tyurin, N.A. Universal Maslov class of a Bohr-Sommerfeld Lagrangian embedding into a pseudo-Einstein manifold. *Theoretical and Mathematical Physics* **150** (2), 278–287 (2007).
- [13] Yoshioka, A. Maslov’s Quantization Conditions for the Bound States of the Hydrogen Atom. *Tokyo J. Math.* **09** (2), 415–437 (1986).
- [14] Czyż, J. On geometric quantization and its connection with the Maslov theory. *Reports of Math. Physics* **15** (1), 57–97 (1979).
- [15] Barilari, D. & Lerario, A. Geometry of Maslov cycles. *Geometric Control Theory and Sub-Riemannian Geometry*. Springer INdAM Series, v.5, 15-35 — (Springer, 2014).
- [16] Borrelli, V. Maslov form and J-volume of totally real immersions. *J. Geom. Phys.* **25** (3-4), 271–290 (1998).
- [17] Littlejohn, R.G. Cyclic evolution in quantum mechanics and the phases of Bohr-Sommerfeld and Maslov. *Phys Rev Lett.* **61**(19), 2159–2162 (1988).
- [18] Chen, B. Y. Maslovian Lagrangian surfaces of constant curvature in complex projective or complex hyperbolic planes *Mathematische Nachrichten* **278** (11), 1242–1281 (2005).
- [19] Yu.E. Pennionzhkevich, *Light Nuclei and Bounds of Neutron Stability*, [in Russian], (OIYaI, Dubna, 2016).
- [20] Gilmore, Robert, Uncertainty relations of statistical mechanics *Phys. Rev. A* **31** (5), 3237–3239 (1985).
- [21] Maslov, V. P. Thermodynamic Concept of Neutron Separation Energy <https://arxiv.org/abs/1812.02586v4> [physics.gen-ph] (2018).
- [22] Maslov, V. P. Case of less than two degrees of freedom, negative pressure, and the Fermi–Dirac distribution for a hard liquid *Math. Notes* **98** (1) 138–157 (2015).
- [23] Bruno, A. D. Self-similar solutions and power geometry *Russian Mathematical Surveys* **55** (1), 1–42 (2000).
- [24] Weinstein, A. The Maslov Gerbe *Letters in Mathematical Physics* **69** (1), 3–9 (2004).
- [25] Maslov, V. P., Myasnikov, V. P. & Danilov V. G. *Mathematical Modeling of the Accident Block of Chernobyl Atomic Station* (Nauka, Moscow, 1987) [in Russian].
- [26] Maslov, V. P. On mathematical investigations related to the Chernobyl disaster. *Russian J. Math. Phys.* **25** (3), 309–318 (2018).
- [27] Maslov, V. P. Statistics corresponding to classical thermodynamics. Construction of isotherms, *Russian J. Math. Phys.*, **22** (1), 53–67 (2015).
- [28] Maslov, V. P. Locally ideal liquid *Russian J. Math. Phys.* **22** (3), 361–373 (2015).
- [29] I. A. Kvasnikov, *Thermodynamics and Statistical Physics: Theory of Equilibrium Systems* (URSS, Moscow, 2003), Vol. 3 [in Russian].

Additional information

Competing interests: The author declares no competing interests.

Appendix

Table 1 is based on the IsotopeData which contains 256 stable elements. The table does not include 2 elements: hydrogen-1 and lithium-3.

Table 1: Parameters for stable isotopes of various nuclei

\mathcal{N}	nucleus	Z	E_b , MeV	δN	$\delta\mu_{min}$	a_0	μ_0 , MeV	$F(a_0)$
1	lead-208	82	1.636*10 ³	2.9672*10 ⁻¹	5.515*10 ³	6.57*10 ⁻¹⁰	-3.46*10 ⁴	1.046203
2	lead-207	82	1.629*10 ³	2.9685*10 ⁻¹	5.488*10 ³	6.7*10 ⁻¹⁰	-3.44*10 ⁴	1.046245
3	lead-206	82	1.622*10 ³	2.9697*10 ⁻¹	5.463*10 ³	6.83*10 ⁻¹⁰	-3.42*10 ⁴	1.046286
4	thallium-205	81	1.615*10 ³	2.971*10 ⁻¹	5.436*10 ³	6.96*10 ⁻¹⁰	-3.41*10 ⁴	1.046328
5	mercury-204	80	1.609*10 ³	2.9723*10 ⁻¹	5.412*10 ³	7.1*10 ⁻¹⁰	-3.39*10 ⁴	1.046369
6	lead-204	82	1.608*10 ³	2.9723*10 ⁻¹	5.408*10 ³	7.11*10 ⁻¹⁰	-3.39*10 ⁴	1.046372
7	thallium-203	81	1.601*10 ³	2.9736*10 ⁻¹	5.384*10 ³	7.25*10 ⁻¹⁰	-3.37*10 ⁴	1.046414
8	mercury-202	80	1.595*10 ³	2.9748*10 ⁻¹	5.362*10 ³	7.38*10 ⁻¹⁰	-3.35*10 ⁴	1.046454
9	mercury-201	80	1.587*10 ³	2.9762*10 ⁻¹	5.334*10 ³	7.54*10 ⁻¹⁰	-3.33*10 ⁴	1.046498
10	mercury-200	80	1.581*10 ³	2.9774*10 ⁻¹	5.311*10 ³	7.68*10 ⁻¹⁰	-3.32*10 ⁴	1.04654
11	mercury-199	80	1.573*10 ³	2.9788*10 ⁻¹	5.281*10 ³	7.85*10 ⁻¹⁰	-3.3*10 ⁴	1.046586
12	platinum-198	78	1.567*10 ³	2.9801*10 ⁻¹	5.258*10 ³	8.*10 ⁻¹⁰	-3.28*10 ⁴	1.046628
13	mercury-198	80	1.566*10 ³	2.9802*10 ⁻¹	5.256*10 ³	8.*10 ⁻¹⁰	-3.28*10 ⁴	1.046629
14	gold-197	79	1.559*10 ³	2.9815*10 ⁻¹	5.23*10 ³	8.17*10 ⁻¹⁰	-3.26*10 ⁴	1.046673
15	platinum-196	78	1.554*10 ³	2.9828*10 ⁻¹	5.209*10 ³	8.33*10 ⁻¹⁰	-3.25*10 ⁴	1.046715
16	mercury-196	80	1.551*10 ³	2.9829*10 ⁻¹	5.2*10 ³	8.35*10 ⁻¹⁰	-3.24*10 ⁴	1.046721
17	platinum-195	78	1.546*10 ³	2.9842*10 ⁻¹	5.18*10 ³	8.51*10 ⁻¹⁰	-3.23*10 ⁴	1.046762
18	platinum-194	78	1.540*10 ³	2.9855*10 ⁻¹	5.157*10 ³	8.68*10 ⁻¹⁰	-3.21*10 ⁴	1.046805
19	iridium-193	77	1.532*10 ³	2.9869*10 ⁻¹	5.129*10 ³	8.86*10 ⁻¹⁰	-3.19*10 ⁴	1.046852
20	osmium-192	76	1.526*10 ³	2.9882*10 ⁻¹	5.107*10 ³	9.04*10 ⁻¹⁰	-3.18*10 ⁴	1.046895
21	platinum-192	78	1.525*10 ³	2.9883*10 ⁻¹	5.103*10 ³	9.05*10 ⁻¹⁰	-3.18*10 ⁴	1.046898
22	iridium-191	77	1.518*10 ³	2.9897*10 ⁻¹	5.078*10 ³	9.24*10 ⁻¹⁰	-3.16*10 ⁴	1.046944
23	osmium-190	76	1.513*10 ³	2.991*10 ⁻¹	5.058*10 ³	9.42*10 ⁻¹⁰	-3.14*10 ⁴	1.046986
24	osmium-189	76	1.505*10 ³	2.9924*10 ⁻¹	5.029*10 ³	9.63*10 ⁻¹⁰	-3.12*10 ⁴	1.047035
25	osmium-188	76	1.499*10 ³	2.9938*10 ⁻¹	5.007*10 ³	9.83*10 ⁻¹⁰	-3.11*10 ⁴	1.047079
26	osmium-187	76	1.491*10 ³	2.9953*10 ⁻¹	4.978*10 ³	1.*10 ⁻⁹	-3.09*10 ⁴	1.047129
27	tungsten-186	74	1.486*10 ³	2.9966*10 ⁻¹	4.959*10 ³	1.02*10 ⁻⁹	-3.08*10 ⁴	1.047173
28	rhenium-185	75	1.478*10 ³	2.9981*10 ⁻¹	4.931*10 ³	1.05*10 ⁻⁹	-3.06*10 ⁴	1.047222
29	tungsten-184	74	1.473*10 ³	2.9994*10 ⁻¹	4.911*10 ³	1.07*10 ⁻⁹	-3.04*10 ⁴	1.047267
30	osmium-184	76	1.470*10 ³	2.9996*10 ⁻¹	4.9*10 ³	1.07*10 ⁻⁹	-3.04*10 ⁴	1.047274
31	tungsten-183	74	1.466*10 ³	3.0009*10 ⁻¹	4.884*10 ³	1.09*10 ⁻⁹	-3.02*10 ⁴	1.047316
32	tungsten-182	74	1.459*10 ³	3.0023*10 ⁻¹	4.861*10 ³	1.12*10 ⁻⁹	-3.01*10 ⁴	1.047363
33	tantalum-181	73	1.452*10 ³	3.0038*10 ⁻¹	4.835*10 ³	1.14*10 ⁻⁹	-2.99*10 ⁴	1.047413
34	hafnium-180	72	1.446*10 ³	3.0052*10 ⁻¹	4.813*10 ³	1.17*10 ⁻⁹	-2.98*10 ⁴	1.04746
35	tungsten-180	74	1.445*10 ³	3.0054*10 ⁻¹	4.807*10 ³	1.17*10 ⁻⁹	-2.97*10 ⁴	1.047465
36	hafnium-179	72	1.439*10 ³	3.0068*10 ⁻¹	4.786*10 ³	1.19*10 ⁻⁹	-2.96*10 ⁴	1.047512
37	hafnium-178	72	1.433*10 ³	3.0082*10 ⁻¹	4.763*10 ³	1.22*10 ⁻⁹	-2.94*10 ⁴	1.04756
38	hafnium-177	72	1.425*10 ³	3.0098*10 ⁻¹	4.735*10 ³	1.25*10 ⁻⁹	-2.92*10 ⁴	1.047612
39	ytterbium-176	70	1.419*10 ³	3.0112*10 ⁻¹	4.713*10 ³	1.27*10 ⁻⁹	-2.91*10 ⁴	1.047661
40	hafnium-176	72	1.419*10 ³	3.0113*10 ⁻¹	4.712*10 ³	1.27*10 ⁻⁹	-2.91*10 ⁴	1.047662
41	lutetium-175	71	1.412*10 ³	3.0128*10 ⁻¹	4.687*10 ³	1.3*10 ⁻⁹	-2.89*10 ⁴	1.047713
42	ytterbium-174	70	1.407*10 ³	3.0143*10 ⁻¹	4.666*10 ³	1.33*10 ⁻⁹	-2.87*10 ⁴	1.047762

\mathcal{N}	nucleus	Z	E_b, MeV	δN	$\delta\mu_{min}$	a_0	μ_0, MeV	$F(a_0)$
43	ytterbium-173	70	1.399*10 ³	3.0159*10 ⁻¹	4.639*10 ³	1.36*10 ⁻⁹	-2.86*10 ⁴	1.047815
44	ytterbium-172	70	1.393*10 ³	3.0174*10 ⁻¹	4.616*10 ³	1.39*10 ⁻⁹	-2.84*10 ⁴	1.047867
45	ytterbium-171	70	1.385*10 ³	3.0191*10 ⁻¹	4.587*10 ³	1.43*10 ⁻⁹	-2.82*10 ⁴	1.047923
46	erbium-170	68	1.379*10 ³	3.0206*10 ⁻¹	4.566*10 ³	1.46*10 ⁻⁹	-2.81*10 ⁴	1.047973
47	ytterbium-170	70	1.378*10 ³	3.0206*10 ⁻¹	4.562*10 ³	1.46*10 ⁻⁹	-2.8*10 ⁴	1.047975
48	thulium-169	69	1.371*10 ³	3.0222*10 ⁻¹	4.538*10 ³	1.5*10 ⁻⁹	-2.79*10 ⁴	1.048029
49	erbium-168	68	1.366*10 ³	3.0237*10 ⁻¹	4.517*10 ³	1.53*10 ⁻⁹	-2.77*10 ⁴	1.04808
50	ytterbium-168	70	1.363*10 ³	3.024*10 ⁻¹	4.507*10 ³	1.53*10 ⁻⁹	-2.77*10 ⁴	1.048088
51	erbium-167	68	1.358*10 ³	3.0254*10 ⁻¹	4.489*10 ³	1.57*10 ⁻⁹	-2.75*10 ⁴	1.048137
52	erbium-166	68	1.352*10 ³	3.0271*10 ⁻¹	4.465*10 ³	1.6*10 ⁻⁹	-2.74*10 ⁴	1.048191
53	holmium-165	67	1.344*10 ³	3.0287*10 ⁻¹	4.438*10 ³	1.64*10 ⁻⁹	-2.72*10 ⁴	1.048248
54	dysprosium-164	66	1.338*10 ³	3.0304*10 ⁻¹	4.415*10 ³	1.68*10 ⁻⁹	-2.7*10 ⁴	1.048302
55	erbium-164	68	1.336*10 ³	3.0305*10 ⁻¹	4.41*10 ³	1.69*10 ⁻⁹	-2.7*10 ⁴	1.048306
56	dysprosium-163	66	1.330*10 ³	3.0321*10 ⁻¹	4.388*10 ³	1.72*10 ⁻⁹	-2.68*10 ⁴	1.04836
57	dysprosium-162	66	1.324*10 ³	3.0337*10 ⁻¹	4.365*10 ³	1.77*10 ⁻⁹	-2.67*10 ⁴	1.048416
58	erbium-162	68	1.321*10 ³	3.034*10 ⁻¹	4.353*10 ³	1.77*10 ⁻⁹	-2.66*10 ⁴	1.048425
59	dysprosium-161	66	1.316*10 ³	3.0355*10 ⁻¹	4.335*10 ³	1.81*10 ⁻⁹	-2.65*10 ⁴	1.048477
60	dysprosium-160	66	1.309*10 ³	3.0372*10 ⁻¹	4.311*10 ³	1.86*10 ⁻⁹	-2.63*10 ⁴	1.048534
61	gadolinium-160	64	1.309*10 ³	3.0372*10 ⁻¹	4.311*10 ³	1.86*10 ⁻⁹	-2.63*10 ⁴	1.048534
62	terbium-159	65	1.302*10 ³	3.039*10 ⁻¹	4.284*10 ³	1.9*10 ⁻⁹	-2.61*10 ⁴	1.048594
63	gadolinium-158	64	1.296*10 ³	3.0407*10 ⁻¹	4.262*10 ³	1.95*10 ⁻⁹	-2.6*10 ⁴	1.04865
64	dysprosium-158	66	1.294*10 ³	3.0408*10 ⁻¹	4.256*10 ³	1.96*10 ⁻⁹	-2.59*10 ⁴	1.048656
65	gadolinium-157	64	1.288*10 ³	3.0425*10 ⁻¹	4.233*10 ³	2.*10 ⁻⁹	-2.58*10 ⁴	1.048713
66	gadolinium-156	64	1.282*10 ³	3.0443*10 ⁻¹	4.21*10 ³	2.05*10 ⁻⁹	-2.56*10 ⁴	1.048771
67	dysprosium-156	66	1.278*10 ³	3.0446*10 ⁻¹	4.198*10 ³	2.06*10 ⁻⁹	-2.56*10 ⁴	1.048782
68	gadolinium-155	64	1.273*10 ³	3.0462*10 ⁻¹	4.179*10 ³	2.11*10 ⁻⁹	-2.54*10 ⁴	1.048837
69	samarium-154	62	1.267*10 ³	3.0479*10 ⁻¹	4.157*10 ³	2.16*10 ⁻⁹	-2.53*10 ⁴	1.048896
70	gadolinium-154	64	1.267*10 ³	3.048*10 ⁻¹	4.156*10 ³	2.16*10 ⁻⁹	-2.53*10 ⁴	1.048896
71	europium-153	63	1.259*10 ³	3.0498*10 ⁻¹	4.128*10 ³	2.22*10 ⁻⁹	-2.51*10 ⁴	1.04896
72	samarium-152	62	1.253*10 ³	3.0516*10 ⁻¹	4.106*10 ³	2.28*10 ⁻⁹	-2.49*10 ⁴	1.049019
73	europium-151	63	1.244*10 ³	3.0536*10 ⁻¹	4.074*10 ³	2.34*10 ⁻⁹	-2.47*10 ⁴	1.049088
74	samarium-150	62	1.239*10 ³	3.0553*10 ⁻¹	4.056*10 ³	2.4*10 ⁻⁹	-2.46*10 ⁴	1.049146
75	samarium-149	62	1.231*10 ³	3.0573*10 ⁻¹	4.027*10 ³	2.47*10 ⁻⁹	-2.44*10 ⁴	1.049213
76	neodymium-148	60	1.225*10 ³	3.0591*10 ⁻¹	4.005*10 ³	2.53*10 ⁻⁹	-2.42*10 ⁴	1.049275
77	neodymium-146	60	1.212*10 ³	3.0628*10 ⁻¹	3.958*10 ³	2.67*10 ⁻⁹	-2.39*10 ⁴	1.049402
78	neodymium-145	60	1.205*10 ³	3.0648*10 ⁻¹	3.931*10 ³	2.74*10 ⁻⁹	-2.38*10 ⁴	1.04947
79	samarium-144	62	1.196*10 ³	3.067*10 ⁻¹	3.899*10 ³	2.83*10 ⁻⁹	-2.35*10 ⁴	1.049544
80	neodymium-143	60	1.191*10 ³	3.0687*10 ⁻¹	3.882*10 ³	2.9*10 ⁻⁹	-2.34*10 ⁴	1.049604
81	cerium-142	58	1.185*10 ³	3.0706*10 ⁻¹	3.86*10 ³	2.97*10 ⁻⁹	-2.33*10 ⁴	1.049669
82	neodymium-142	60	1.185*10 ³	3.0706*10 ⁻¹	3.86*10 ³	2.97*10 ⁻⁹	-2.33*10 ⁴	1.049669
83	praseodymium-141	59	1.178*10 ³	3.0727*10 ⁻¹	3.834*10 ³	3.06*10 ⁻⁹	-2.31*10 ⁴	1.049739
84	cerium-140	58	1.173*10 ³	3.0745*10 ⁻¹	3.814*10 ³	3.14*10 ⁻⁹	-2.3*10 ⁴	1.049803
85	lanthanum-139	57	1.165*10 ³	3.0767*10 ⁻¹	3.785*10 ³	3.23*10 ⁻⁹	-2.28*10 ⁴	1.049877
86	barium-138	56	1.158*10 ³	3.0787*10 ⁻¹	3.762*10 ³	3.33*10 ⁻⁹	-2.26*10 ⁴	1.049946
87	cerium-138	58	1.156*10 ³	3.0789*10 ⁻¹	3.755*10 ³	3.34*10 ⁻⁹	-2.26*10 ⁴	1.049953
88	barium-137	56	1.150*10 ³	3.0809*10 ⁻¹	3.732*10 ³	3.43*10 ⁻⁹	-2.24*10 ⁴	1.050023
89	barium-136	56	1.143*10 ³	3.083*10 ⁻¹	3.707*10 ³	3.53*10 ⁻⁹	-2.22*10 ⁴	1.050095
90	xenon-136	54	1.142*10 ³	3.0831*10 ⁻¹	3.704*10 ³	3.53*10 ⁻⁹	-2.22*10 ⁴	1.050098

\mathcal{N}	nucleus	Z	E_b, MeV	δN	$\delta\mu_{min}$	a_0	μ_0, MeV	$F(a_0)$
91	cerium-136	58	1.139*10 ³	3.0834*10 ⁻¹	3.693*10 ³	3.55*10 ⁻⁹	-2.22*10 ⁴	1.050109
92	barium-135	56	1.134*10 ³	3.0854*10 ⁻¹	3.674*10 ³	3.64*10 ⁻⁹	-2.2*10 ⁴	1.050176
93	xenon-134	54	1.127*10 ³	3.0875*10 ⁻¹	3.652*10 ³	3.75*10 ⁻⁹	-2.19*10 ⁴	1.050247
94	barium-134	56	1.127*10 ³	3.0875*10 ⁻¹	3.649*10 ³	3.75*10 ⁻⁹	-2.19*10 ⁴	1.050249
95	cesium-133	55	1.119*10 ³	3.0898*10 ⁻¹	3.62*10 ³	3.87*10 ⁻⁹	-2.17*10 ⁴	1.050328
96	xenon-132	54	1.112*10 ³	3.0919*10 ⁻¹	3.598*10 ³	3.98*10 ⁻⁹	-2.15*10 ⁴	1.050401
97	barium-132	56	1.110*10 ³	3.0922*10 ⁻¹	3.59*10 ³	4.*10 ⁻⁹	-2.15*10 ⁴	1.050409
98	xenon-131	54	1.104*10 ³	3.0943*10 ⁻¹	3.566*10 ³	4.12*10 ⁻⁹	-2.13*10 ⁴	1.050484
99	xenon-130	54	1.097*10 ³	3.0965*10 ⁻¹	3.542*10 ³	4.24*10 ⁻⁹	-2.11*10 ⁴	1.05056
100	barium-130	56	1.093*10 ³	3.097*10 ⁻¹	3.528*10 ³	4.27*10 ⁻⁹	-2.11*10 ⁴	1.050575
101	xenon-129	54	1.088*10 ³	3.099*10 ⁻¹	3.51*10 ³	4.39*10 ⁻⁹	-2.09*10 ⁴	1.050646
102	xenon-128	54	1.081*10 ³	3.1013*10 ⁻¹	3.485*10 ³	4.52*10 ⁻⁹	-2.08*10 ⁴	1.050725
103	iodine-127	53	1.073*10 ³	3.1037*10 ⁻¹	3.456*10 ³	4.67*10 ⁻⁹	-2.06*10 ⁴	1.050809
104	tellurium-126	52	1.066*10 ³	3.1059*10 ⁻¹	3.433*10 ³	4.81*10 ⁻⁹	-2.04*10 ⁴	1.050886
105	xenon-126	54	1.064*10 ³	3.1062*10 ⁻¹	3.425*10 ³	4.83*10 ⁻⁹	-2.04*10 ⁴	1.050896
106	tellurium-125	52	1.057*10 ³	3.1085*10 ⁻¹	3.401*10 ³	4.98*10 ⁻⁹	-2.02*10 ⁴	1.050976
107	tellurium-124	52	1.051*10 ³	3.1108*10 ⁻¹	3.377*10 ³	5.14*10 ⁻⁹	-2.01*10 ⁴	1.051057
108	tin-124	50	1.050*10 ³	3.1109*10 ⁻¹	3.375*10 ³	5.15*10 ⁻⁹	-2.*10 ⁴	1.051059
109	xenon-124	54	1.046*10 ³	3.1113*10 ⁻¹	3.363*10 ³	5.17*10 ⁻⁹	-2.*10 ⁴	1.051074
110	antimony-123	51	1.042*10 ³	3.1134*10 ⁻¹	3.347*10 ³	5.32*10 ⁻⁹	-1.99*10 ⁴	1.051146
111	tin-122	50	1.036*10 ³	3.1158*10 ⁻¹	3.323*10 ³	5.49*10 ⁻⁹	-1.97*10 ⁴	1.051229
112	tellurium-122	52	1.034*10 ³	3.1159*10 ⁻¹	3.32*10 ³	5.5*10 ⁻⁹	-1.97*10 ⁴	1.051234
113	antimony-121	51	1.026*10 ³	3.1185*10 ⁻¹	3.291*10 ³	5.69*10 ⁻⁹	-1.95*10 ⁴	1.051323
114	tin-120	50	1.021*10 ³	3.1208*10 ⁻¹	3.27*10 ³	5.87*10 ⁻⁹	-1.93*10 ⁴	1.051404
115	tellurium-120	52	1.017*10 ³	3.1212*10 ⁻¹	3.259*10 ³	5.9*10 ⁻⁹	-1.93*10 ⁴	1.051418
116	tin-119	50	1.011*10 ³	3.1236*10 ⁻¹	3.238*10 ³	6.08*10 ⁻⁹	-1.91*10 ⁴	1.0515
117	tin-118	50	1.005*10 ³	3.126*10 ⁻¹	3.215*10 ³	6.29*10 ⁻⁹	-1.9*10 ⁴	1.051586
118	tin-117	50	995.6	3.1289*10 ⁻¹	3.182*10 ³	6.52*10 ⁻⁹	-1.88*10 ⁴	1.051685
119	tin-116	50	988.7	3.1314*10 ⁻¹	3.157*10 ³	6.75*10 ⁻⁹	-1.86*10 ⁴	1.051775
120	tin-115	50	979.1	3.1343*10 ⁻¹	3.124*10 ³	7.01*10 ⁻⁹	-1.84*10 ⁴	1.051878
121	cadmium-114	48	972.6	3.1369*10 ⁻¹	3.1*10 ³	7.25*10 ⁻⁹	-1.82*10 ⁴	1.051969
122	tin-114	50	971.6	3.1371*10 ⁻¹	3.097*10 ³	7.26*10 ⁻⁹	-1.82*10 ⁴	1.051973
123	indium-113	49	963.1	3.1399*10 ⁻¹	3.067*10 ³	7.54*10 ⁻⁹	-1.8*10 ⁴	1.052074
124	cadmium-112	48	957.0	3.1425*10 ⁻¹	3.045*10 ³	7.79*10 ⁻⁹	-1.79*10 ⁴	1.052165
125	tin-112	50	953.5	3.1429*10 ⁻¹	3.034*10 ³	7.84*10 ⁻⁹	-1.78*10 ⁴	1.05218
126	cadmium-111	48	947.6	3.1455*10 ⁻¹	3.013*10 ³	8.1*10 ⁻⁹	-1.77*10 ⁴	1.052272
127	cadmium-110	48	940.6	3.1483*10 ⁻¹	2.988*10 ³	8.4*10 ⁻⁹	-1.75*10 ⁴	1.052369
128	palladium-110	46	940.2	3.1483*10 ⁻¹	2.986*10 ³	8.4*10 ⁻⁹	-1.75*10 ⁴	1.052371
129	silver-109	47	931.7	3.1513*10 ⁻¹	2.957*10 ³	8.73*10 ⁻⁹	-1.73*10 ⁴	1.052477
130	palladium-108	46	925.2	3.1541*10 ⁻¹	2.933*10 ³	9.05*10 ⁻⁹	-1.71*10 ⁴	1.052574
131	cadmium-108	48	923.4	3.1543*10 ⁻¹	2.927*10 ³	9.08*10 ⁻⁹	-1.71*10 ⁴	1.052583
132	silver-107	47	915.3	3.1574*10 ⁻¹	2.899*10 ³	9.43*10 ⁻⁹	-1.69*10 ⁴	1.05269
133	palladium-106	46	909.5	3.1601*10 ⁻¹	2.878*10 ³	9.77*10 ⁻⁹	-1.68*10 ⁴	1.052787
134	cadmium-106	48	905.1	3.1607*10 ⁻¹	2.864*10 ³	9.84*10 ⁻⁹	-1.67*10 ⁴	1.052808
135	palladium-105	46	899.9	3.1634*10 ⁻¹	2.845*10 ³	1.02*10 ⁻⁸	-1.66*10 ⁴	1.052903
136	ruthenium-104	44	893.1	3.1663*10 ⁻¹	2.821*10 ³	1.06*10 ⁻⁸	-1.64*10 ⁴	1.053008
137	palladium-104	46	892.8	3.1663*10 ⁻¹	2.82*10 ³	1.06*10 ⁻⁸	-1.64*10 ⁴	1.053009
138	rhodium-103	45	884.2	3.1696*10 ⁻¹	2.79*10 ³	1.1*10 ⁻⁸	-1.62*10 ⁴	1.053125

\mathcal{N}	nucleus	Z	E_b, MeV	δN	$\delta\mu_{min}$	a_0	μ_0, MeV	$F(a_0)$
139	ruthenium-102	44	877.9	$3.1725*10^{-1}$	$2.767*10^3$	$1.14*10^{-8}$	$-1.61*10^4$	1.053229
140	palladium-102	46	875.2	$3.1729*10^{-1}$	$2.758*10^3$	$1.15*10^{-8}$	$-1.6*10^4$	1.053243
141	ruthenium-101	44	868.7	$3.1759*10^{-1}$	$2.735*10^3$	$1.19*10^{-8}$	$-1.58*10^4$	1.05335
142	ruthenium-100	44	861.9	$3.179*10^{-1}$	$2.711*10^3$	$1.24*10^{-8}$	$-1.57*10^4$	1.053461
143	ruthenium-99	44	852.3	$3.1826*10^{-1}$	$2.678*10^3$	$1.3*10^{-8}$	$-1.55*10^4$	1.053588
144	molybdenum-98	42	846.2	$3.1856*10^{-1}$	$2.656*10^3$	$1.35*10^{-8}$	$-1.53*10^4$	1.053698
145	ruthenium-98	44	844.8	$3.1858*10^{-1}$	$2.652*10^3$	$1.35*10^{-8}$	$-1.53*10^4$	1.053705
146	molybdenum-97	42	837.6	$3.1891*10^{-1}$	$2.626*10^3$	$1.41*10^{-8}$	$-1.51*10^4$	1.053823
147	molybdenum-96	42	830.8	$3.1924*10^{-1}$	$2.602*10^3$	$1.46*10^{-8}$	$-1.5*10^4$	1.05394
148	ruthenium-96	44	826.5	$3.193*10^{-1}$	$2.588*10^3$	$1.48*10^{-8}$	$-1.49*10^4$	1.053964
149	molybdenum-95	42	821.6	$3.196*10^{-1}$	$2.571*10^3$	$1.53*10^{-8}$	$-1.48*10^4$	1.054072
150	zirconium-94	40	814.7	$3.1994*10^{-1}$	$2.546*10^3$	$1.6*10^{-8}$	$-1.46*10^4$	1.054193
151	molybdenum-94	42	814.3	$3.1995*10^{-1}$	$2.545*10^3$	$1.6*10^{-8}$	$-1.46*10^4$	1.054196
152	niobium-93	41	805.8	$3.2031*10^{-1}$	$2.516*10^3$	$1.67*10^{-8}$	$-1.44*10^4$	1.054328
153	zirconium-92	40	799.7	$3.2065*10^{-1}$	$2.494*10^3$	$1.74*10^{-8}$	$-1.43*10^4$	1.054448
154	molybdenum-92	42	796.5	$3.207*10^{-1}$	$2.484*10^3$	$1.75*10^{-8}$	$-1.42*10^4$	1.054467
155	zirconium-91	40	791.1	$3.2103*10^{-1}$	$2.464*10^3$	$1.82*10^{-8}$	$-1.41*10^4$	1.054585
156	zirconium-90	40	783.9	$3.2139*10^{-1}$	$2.439*10^3$	$1.9*10^{-8}$	$-1.39*10^4$	1.054716
157	yttrium-89	39	775.5	$3.2177*10^{-1}$	$2.41*10^3$	$2.*10^{-8}$	$-1.38*10^4$	1.054855
158	strontium-88	38	768.5	$3.2214*10^{-1}$	$2.386*10^3$	$2.09*10^{-8}$	$-1.36*10^4$	1.054989
159	strontium-87	38	757.4	$3.2258*10^{-1}$	$2.348*10^3$	$2.2*10^{-8}$	$-1.34*10^4$	1.055151
160	krypton-86	36	749.2	$3.2298*10^{-1}$	$2.32*10^3$	$2.31*10^{-8}$	$-1.32*10^4$	1.055297
161	strontium-86	38	748.9	$3.2299*10^{-1}$	$2.319*10^3$	$2.31*10^{-8}$	$-1.32*10^4$	1.055299
162	rubidium-85	37	739.3	$3.2342*10^{-1}$	$2.286*10^3$	$2.43*10^{-8}$	$-1.3*10^4$	1.055457
163	krypton-84	36	732.3	$3.2381*10^{-1}$	$2.261*10^3$	$2.55*10^{-8}$	$-1.28*10^4$	1.0556
164	strontium-84	38	728.9	$3.2388*10^{-1}$	$2.251*10^3$	$2.57*10^{-8}$	$-1.27*10^4$	1.055623
165	krypton-83	36	721.7	$3.2428*10^{-1}$	$2.226*10^3$	$2.69*10^{-8}$	$-1.26*10^4$	1.05577
166	krypton-82	36	714.3	$3.2469*10^{-1}$	$2.2*10^3$	$2.82*10^{-8}$	$-1.24*10^4$	1.055921
167	bromine-81	35	704.4	$3.2516*10^{-1}$	$2.166*10^3$	$2.98*10^{-8}$	$-1.22*10^4$	1.056093
168	selenium-80	34	696.9	$3.2558*10^{-1}$	$2.14*10^3$	$3.14*10^{-8}$	$-1.2*10^4$	1.05625
169	krypton-80	36	695.4	$3.2561*10^{-1}$	$2.136*10^3$	$3.15*10^{-8}$	$-1.2*10^4$	1.056261
170	bromine-79	35	686.3	$3.2608*10^{-1}$	$2.105*10^3$	$3.32*10^{-8}$	$-1.18*10^4$	1.056433
171	selenium-78	34	680.0	$3.265*10^{-1}$	$2.083*10^3$	$3.49*10^{-8}$	$-1.17*10^4$	1.056588
172	krypton-78	36	675.6	$3.2659*10^{-1}$	$2.069*10^3$	$3.52*10^{-8}$	$-1.16*10^4$	1.056621
173	selenium-77	34	669.5	$3.2701*10^{-1}$	$2.047*10^3$	$3.7*10^{-8}$	$-1.15*10^4$	1.056777
174	selenium-76	34	662.1	$3.2747*10^{-1}$	$2.022*10^3$	$3.9*10^{-8}$	$-1.13*10^4$	1.056947
175	arsenic-75	33	652.6	$3.2797*10^{-1}$	$1.99*10^3$	$4.13*10^{-8}$	$-1.11*10^4$	1.057136
176	germanium-74	32	645.7	$3.2844*10^{-1}$	$1.966*10^3$	$4.35*10^{-8}$	$-1.09*10^4$	1.057308
177	selenium-74	34	642.9	$3.285*10^{-1}$	$1.957*10^3$	$4.38*10^{-8}$	$-1.09*10^4$	1.05733
178	germanium-73	32	635.5	$3.2898*10^{-1}$	$1.932*10^3$	$4.63*10^{-8}$	$-1.07*10^4$	1.05751
179	germanium-72	32	628.7	$3.2945*10^{-1}$	$1.908*10^3$	$4.88*10^{-8}$	$-1.06*10^4$	1.057688
180	gallium-71	31	619.0	$3.3001*10^{-1}$	$1.876*10^3$	$5.2*10^{-8}$	$-1.04*10^4$	1.057895
181	zinc-70	30	611.1	$3.3053*10^{-1}$	$1.849*10^3$	$5.51*10^{-8}$	$-1.02*10^4$	1.05809
182	germanium-70	32	610.5	$3.3054*10^{-1}$	$1.847*10^3$	$5.52*10^{-8}$	$-1.02*10^4$	1.058095
183	gallium-69	31	602.0	$3.3108*10^{-1}$	$1.818*10^3$	$5.86*10^{-8}$	$-1.*10^4$	1.0583
184	zinc-68	30	595.4	$3.3159*10^{-1}$	$1.796*10^3$	$6.2*10^{-8}$	$-9.88*10^3$	1.058492
185	zinc-67	30	585.2	$3.322*10^{-1}$	$1.762*10^3$	$6.63*10^{-8}$	$-9.67*10^3$	1.058722
186	zinc-66	30	578.1	$3.3274*10^{-1}$	$1.737*10^3$	$7.03*10^{-8}$	$-9.52*10^3$	1.058927

\mathcal{N}	nucleus	Z	E_b, MeV	δN	$\delta\mu_{min}$	a_0	μ_0, MeV	$F(a_0)$
187	copper-65	29	569.2	$3.3334*10^{-1}$	$1.708*10^3$	$7.51*10^{-8}$	$-9.34*10^3$	1.059155
188	nickel-64	28	561.8	$3.3392*10^{-1}$	$1.682*10^3$	$7.99*10^{-8}$	$-9.18*10^3$	1.059374
189	zinc-64	30	559.1	$3.3399*10^{-1}$	$1.674*10^3$	$8.05*10^{-8}$	$-9.13*10^3$	1.0594
190	copper-63	29	551.4	$3.3458*10^{-1}$	$1.648*10^3$	$8.58*10^{-8}$	$-8.97*10^3$	1.059627
191	nickel-62	28	545.3	$3.3514*10^{-1}$	$1.627*10^3$	$9.12*10^{-8}$	$-8.84*10^3$	1.059842
192	nickel-61	28	534.7	$3.3584*10^{-1}$	$1.592*10^3$	$9.82*10^{-8}$	$-8.63*10^3$	1.060111
193	nickel-60	28	526.8	$3.3648*10^{-1}$	$1.566*10^3$	$1.05*10^{-7}$	$-8.47*10^3$	1.060355
194	cobalt-59	27	517.3	$3.3718*10^{-1}$	$1.534*10^3$	$1.13*10^{-7}$	$-8.27*10^3$	1.060626
195	iron-58	26	509.9	$3.3784*10^{-1}$	$1.509*10^3$	$1.21*10^{-7}$	$-8.12*10^3$	1.060878
196	nickel-58	28	506.5	$3.3794*10^{-1}$	$1.499*10^3$	$1.22*10^{-7}$	$-8.06*10^3$	1.060919
197	iron-57	26	499.9	$3.3859*10^{-1}$	$1.476*10^3$	$1.31*10^{-7}$	$-7.92*10^3$	1.061169
198	iron-56	26	492.3	$3.3928*10^{-1}$	$1.451*10^3$	$1.41*10^{-7}$	$-7.77*10^3$	1.061439
199	manganese-55	25	482.1	$3.4007*10^{-1}$	$1.418*10^3$	$1.53*10^{-7}$	$-7.57*10^3$	1.061748
200	chromium-54	24	474.0	$3.4082*10^{-1}$	$1.391*10^3$	$1.65*10^{-7}$	$-7.4*10^3$	1.062038
201	iron-54	26	471.8	$3.4089*10^{-1}$	$1.384*10^3$	$1.66*10^{-7}$	$-7.36*10^3$	1.062067
202	chromium-53	24	464.3	$3.4163*10^{-1}$	$1.359*10^3$	$1.79*10^{-7}$	$-7.21*10^3$	1.062359
203	chromium-52	24	456.3	$3.4241*10^{-1}$	$1.333*10^3$	$1.94*10^{-7}$	$-7.05*10^3$	1.062665
204	vanadium-51	23	445.8	$3.433*10^{-1}$	$1.299*10^3$	$2.12*10^{-7}$	$-6.85*10^3$	1.063017
205	titanium-50	22	437.8	$3.4413*10^{-1}$	$1.272*10^3$	$2.3*10^{-7}$	$-6.69*10^3$	1.063345
206	chromium-50	24	435.0	$3.4423*10^{-1}$	$1.264*10^3$	$2.32*10^{-7}$	$-6.65*10^3$	1.063385
207	titanium-49	22	426.8	$3.4509*10^{-1}$	$1.237*10^3$	$2.52*10^{-7}$	$-6.48*10^3$	1.063726
208	titanium-48	22	418.7	$3.4597*10^{-1}$	$1.21*10^3$	$2.75*10^{-7}$	$-6.32*10^3$	1.064077
209	titanium-47	22	407.1	$3.4702*10^{-1}$	$1.173*10^3$	$3.04*10^{-7}$	$-6.11*10^3$	1.064496
210	calcium-46	20	398.8	$3.4796*10^{-1}$	$1.146*10^3$	$3.33*10^{-7}$	$-5.95*10^3$	1.064875
211	titanium-46	22	398.2	$3.4799*10^{-1}$	$1.144*10^3$	$3.34*10^{-7}$	$-5.94*10^3$	1.064885
212	scandium-45	21	387.8	$3.4905*10^{-1}$	$1.111*10^3$	$3.7*10^{-7}$	$-5.74*10^3$	1.065313
213	calcium-44	20	381.0	$3.4999*10^{-1}$	$1.088*10^3$	$4.04*10^{-7}$	$-5.61*10^3$	1.065694
214	calcium-43	20	369.8	$3.5116*10^{-1}$	$1.053*10^3$	$4.51*10^{-7}$	$-5.4*10^3$	1.066168
215	calcium-42	20	361.9	$3.5221*10^{-1}$	$1.027*10^3$	$4.97*10^{-7}$	$-5.25*10^3$	1.0666
216	potassium-41	19	351.6	$3.5342*10^{-1}$	$9.949*10^2$	$5.55*10^{-7}$	$-5.06*10^3$	1.067095
217	argon-40	18	343.8	$3.5455*10^{-1}$	$9.697*10^2$	$6.15*10^{-7}$	$-4.92*10^3$	1.067559
218	calcium-40	20	342.1	$3.5464*10^{-1}$	$9.645*10^2$	$6.2*10^{-7}$	$-4.89*10^3$	1.067596
219	potassium-39	19	333.7	$3.5583*10^{-1}$	$9.379*10^2$	$6.9*10^{-7}$	$-4.73*10^3$	1.068092
220	argon-38	18	327.3	$3.5696*10^{-1}$	$9.17*10^2$	$7.64*10^{-7}$	$-4.61*10^3$	1.068562
221	chlorine-37	17	317.1	$3.5836*10^{-1}$	$8.849*10^2$	$8.63*10^{-7}$	$-4.43*10^3$	1.069144
222	sulfur-36	16	308.7	$3.597*10^{-1}$	$8.583*10^2$	$9.7*10^{-7}$	$-4.27*10^3$	1.069707
223	argon-36	18	306.7	$3.5982*10^{-1}$	$8.524*10^2$	$9.81*10^{-7}$	$-4.24*10^3$	1.069758
224	chlorine-35	17	298.2	$3.6123*10^{-1}$	$8.256*10^2$	$1.11*10^{-6}$	$-4.09*10^3$	1.070352
225	sulfur-34	16	291.8	$3.6255*10^{-1}$	$8.05*10^2$	$1.24*10^{-6}$	$-3.97*10^3$	1.070915
226	sulfur-33	16	280.4	$3.6427*10^{-1}$	$7.698*10^2$	$1.43*10^{-6}$	$-3.77*10^3$	1.071651
227	sulfur-32	16	271.8	$3.6588*10^{-1}$	$7.428*10^2$	$1.64*10^{-6}$	$-3.62*10^3$	1.072343
228	phosphorus-31	15	262.9	$3.6758*10^{-1}$	$7.153*10^2$	$1.88*10^{-6}$	$-3.47*10^3$	1.073079
229	silicon-30	14	255.6	$3.6924*10^{-1}$	$6.923*10^2$	$2.15*10^{-6}$	$-3.34*10^3$	1.073802
230	silicon-29	14	245.0	$3.7126*10^{-1}$	$6.599*10^2$	$2.52*10^{-6}$	$-3.16*10^3$	1.074685
231	silicon-28	14	236.5	$3.732*10^{-1}$	$6.338*10^2$	$2.94*10^{-6}$	$-3.01*10^3$	1.075542
232	aluminum-27	13	225.0	$3.7553*10^{-1}$	$5.99*10^2$	$3.52*10^{-6}$	$-2.82*10^3$	1.076583
233	magnesium-26	12	216.7	$3.7769*10^{-1}$	$5.737*10^2$	$4.14*10^{-6}$	$-2.69*10^3$	1.077551
234	magnesium-25	12	205.6	$3.8027*10^{-1}$	$5.406*10^2$	$5.02*10^{-6}$	$-2.51*10^3$	1.078722

\mathcal{N}	nucleus	\mathcal{Z}	E_b, MeV	δN	$\delta \mu_{min}$	a_0	μ_0, MeV	$F(a_0)$
235	magnesium-24	12	198.3	$3.826 \cdot 10^{-1}$	$5.182 \cdot 10^2$	$5.95 \cdot 10^{-6}$	$-2.39 \cdot 10^3$	1.07979
236	sodium-23	11	186.6	$3.8561 \cdot 10^{-1}$	$4.838 \cdot 10^2$	$7.37 \cdot 10^{-6}$	$-2.2 \cdot 10^3$	1.081181
237	neon-22	10	177.8	$3.8847 \cdot 10^{-1}$	$4.576 \cdot 10^2$	$9 \cdot 10^{-6}$	$-2.07 \cdot 10^3$	1.08252
238	neon-21	10	167.4	$3.9178 \cdot 10^{-1}$	$4.273 \cdot 10^2$	$1.13 \cdot 10^{-5}$	$-1.91 \cdot 10^3$	1.084081
239	neon-20	10	160.6	$3.9479 \cdot 10^{-1}$	$4.069 \cdot 10^2$	$1.38 \cdot 10^{-5}$	$-1.8 \cdot 10^3$	1.085525
240	fluorine-19	9	147.8	$3.9907 \cdot 10^{-1}$	$3.704 \cdot 10^2$	$1.82 \cdot 10^{-5}$	$-1.61 \cdot 10^3$	1.0876
241	oxygen-18	8	139.8	$4.0288 \cdot 10^{-1}$	$3.47 \cdot 10^2$	$2.31 \cdot 10^{-5}$	$-1.49 \cdot 10^3$	1.089478
242	oxygen-17	8	131.8	$4.0704 \cdot 10^{-1}$	$3.237 \cdot 10^2$	$2.98 \cdot 10^{-5}$	$-1.37 \cdot 10^3$	1.091564
243	oxygen-16	8	127.6	$4.1074 \cdot 10^{-1}$	$3.107 \cdot 10^2$	$3.72 \cdot 10^{-5}$	$-1.3 \cdot 10^3$	1.093442
244	nitrogen-15	7	115.5	$4.1673 \cdot 10^{-1}$	$2.771 \cdot 10^2$	$5.24 \cdot 10^{-5}$	$-1.14 \cdot 10^3$	1.096538
245	nitrogen-14	7	104.7	$4.2319 \cdot 10^{-1}$	$2.473 \cdot 10^2$	$7.48 \cdot 10^{-5}$	$-9.94 \cdot 10^2$	1.099958
246	carbon-13	6	97.11	$4.2948 \cdot 10^{-1}$	$2.261 \cdot 10^2$	$1.04 \cdot 10^{-4}$	$-8.9 \cdot 10^2$	1.103371
247	carbon-12	6	92.16	$4.3565 \cdot 10^{-1}$	$2.116 \cdot 10^2$	$1.42 \cdot 10^{-4}$	$-8.16 \cdot 10^2$	1.106795
248	boron-11	5	76.20	$4.4753 \cdot 10^{-1}$	$1.703 \cdot 10^2$	$2.5 \cdot 10^{-4}$	$-6.32 \cdot 10^2$	1.113615
249	boron-10	5	64.75	$4.5996 \cdot 10^{-1}$	$1.408 \cdot 10^2$	$4.32 \cdot 10^{-4}$	$-5.02 \cdot 10^2$	1.121078
250	beryllium-9	4	58.16	$4.7184 \cdot 10^{-1}$	$1.233 \cdot 10^2$	$7.01 \cdot 10^{-4}$	$-4.22 \cdot 10^2$	1.128538
251	lithium-7	3	39.24	$5.1231 \cdot 10^{-1}$	$7.66 \cdot 10^1$	$2.9 \cdot 10^{-3}$	$-2.29 \cdot 10^2$	1.156422
252	lithium-6	3	31.99	$5.4087 \cdot 10^{-1}$	$5.915 \cdot 10^1$	$6.64 \cdot 10^{-3}$	$-1.6 \cdot 10^2$	1.178496
253	helium-4	2	28.30	$6.0521 \cdot 10^{-1}$	$4.675 \cdot 10^1$	$2.98 \cdot 10^{-2}$	$-9.94 \cdot 10^1$	1.235472
254	deuterium	1	2.225	2.6432	$8.416 \cdot 10^{-1}$	$1.42 \cdot 10^5$	$2.64 \cdot 10^1$	5.069582

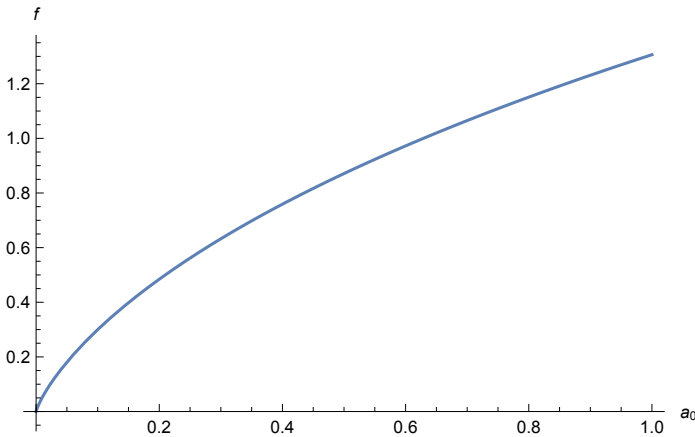


Figure 6: The dependence of the left hand side of the equation (60) on a_0

Here \mathcal{Z} is the charge number (number of protons) in the nucleus and E_b is the binding energy of the nucleus, equal to the core temperature T . It is well known that the binding energy of a nucleus increases with increasing mass number A . At the same time, the mass of the nucleus m and its volume V also grow. The equation (50) for $\gamma = 1/2$ can be written as follows:

$$\frac{1}{2} \text{Li}_{3/2}(a_0) - \log(a_0) \text{Li}_{1/2}(a_0) = \frac{1}{V} \left(\frac{2\pi\hbar^2}{mT} \right)^{3/2}. \quad (60)$$

The value $a = a_0$ is the minimum value of activity for the Bose branch, since for $a < a_0$ the region of uncertainty occurs where $N \equiv 0$ and $P \equiv 0$ for all a up to the value of $a = 0$. Here the passage to the Fermi branch begins. Hence a_0 is the point separating the Bose case from the case of uncertainty.

The left hand side of Eq. (60) which we denote by $f(a_0)$ decreases when the value of a_0 decreases (see Fig. 6). The value in the right hand side of (60) also decreases with the growth of the nucleus mass number A .

Therefore, as one can see from the Table, the activity a_0 decreases and the absolute value of the chemical potential $|\mu_0| = T|\log a_0|$ increases when the mass number A increases.

The variance of the particle number $(\overline{\Delta N})^2$ for given variables μ, V, T in a grand canonical ensemble is determined by the relation (see [29]):

$$\overline{(\Delta N)^2} = T \left(\frac{\partial N}{\partial \mu} \right)_T. \quad (61)$$

By differentiating with respect to μ the both sides of the relation

$$N(\mu, V, T) = \frac{V}{\lambda^D} (\text{Li}_{1+\gamma}(a) - \frac{1}{(N(\mu, V, T) + 1)^\gamma} \text{Li}_{1+\gamma}(a^{N(\mu, V, T)+1})), \quad (62)$$

we obtain the relation for $\left(\frac{\partial N}{\partial \mu} \right)_T$:

$$\left(\frac{\partial N}{\partial \mu} \right)_T = \frac{(N+1)^{\gamma+1} \left(-(N+1)^{1-\gamma} \text{Li}_\gamma \left((e^{\mu/T})^{N+1} \right) + \text{Li}_\gamma \left(e^{\mu/T} \right) \right)}{T \left(\frac{\lambda^{\gamma+1}}{V} (N+1)^{\gamma+1} - \gamma \text{Li}_{\gamma+1} \left((e^{\mu/T})^{N+1} \right) + (N+1) \log(e^{\mu/T}) \text{Li}_\gamma \left((e^{\mu/T})^{N+1} \right) \right)}, \quad (63)$$

where $N = N(\mu, V, T)$.

The expression for dispersion for small N in the zeroth approximation has the form

$$\overline{(\Delta N)^2} = -2 \frac{(1-\gamma) \text{Li}_\gamma(a_0) + \log(a_0) \text{Li}_{\gamma-1}(a_0)}{\log^2(a) \text{Li}_{\gamma-1}(a_0) + \gamma((\gamma+1) \text{Li}_{\gamma+1}(a_0) - 2 \log(a_0) \text{Li}_\gamma(a_0))}. \quad (64)$$

Let us denote for arbitrary value x its mean square fluctuation by $\delta x = \sqrt{(\overline{\Delta x})^2}$. Using a well-known for a grand canonical ensemble relation of uncertainty $\delta N \delta \mu \geq T$, one can find the minimum value of mean square fluctuation $\delta \mu_{min} = T/\delta N \leq \delta \mu$.

The values $\delta \mu_{min}$ (in MeV) and δN are presented on the Table above.

The value $\delta \mu$ determines the halo width and monotonically changes with all columns of the Table.

Thus we have obtained a new table for nuclear physics which demonstrates a monotonic relation between the nucleus mass number A , the binding energy E_b , the minimum value of activity $a = a_0$, the chemical potential $\mu_0 = T \log a_0$, the compressibility factor $F = PV/NT$ for a_0 , and also the minimum value of mean square fluctuation $\delta \mu_{min} = T/\delta N \leq \delta \mu$. The values $\delta \mu_{min}$ and δN are involved in uncertainty relations of nuclear physics.